Hindawi
Mathematical Problems in Engineering
Volume 2019, Article ID 2416342, 13 pages
https://doi.org/10.1155/2019/2416342

Research Article

An Optimization Design Method of Combination of Steep Slope and Sharp Curve Sections for Mountain Highways

Lei Yue [1] **and Hui Wang** [2]

[1] *The Key Laboratory of Road and Traffic Engineering, Ministry of Education at Tongji University, Shanghai 201804, China*
[2] *School of Civil Engineering, Chongqing University, Chongqing 400045, China*

Correspondence should be addressed to Hui Wang; mickysophy@cqu.edu.cn

Received 22 October 2018; Revised 23 January 2019; Accepted 17 February 2019; Published 5 March 2019

Academic Editor: Alexander Paz

As it was found steep slope and sharp curve sections account for 14% of the accident-prone sections according to the accidents data in Chongqing. Regular design indices with certain thresholds are found not enough for this kind of mountain highways. The goal of this paper is to find an optimization design method for combination of steep slope and sharp curve sections based on the analysis of vehicle driving stability. The overall safety model of steep slope and sharp curve combined section is established, and the relevant coordination relationship between design indices of the front and rear alignment unit is established by using the operating speed estimation model. Taking the maximum slope length corresponding to the specified design speed as the design condition of the front segment, the threshold values and variation rules of the design indices of the rear segment under different design speeds are calculated ensuring driving safety. The safety model is simulated by CarSim software, the trajectory offset and lateral acceleration are used to indirectly reflect the degree of lateral instability, and the results are compared to verify the effectiveness of the simplified safety model established in this paper.

1. Introduction

According to the statistical analysis of 1448 traffic accidents on the highways in Chongqing mountainous area [1], 45% of the accidents were caused by overturning, and combination of steep slope and sharp curve (SSSC) sections accounts for 14% of the accident-prone sections. The design standard has not given enough consideration of this condition (SSSC) [2]. Moreover, the safety evaluation standard provides the minimum radius from another perspective [3], which is not adaptable to be used directly for design.

Xu et al. pointed that the design speed method becomes less applicable or even invalid for lower-speed expressways through mountainous areas, since the driving conditions are fundamentally different [4]. Researchers have found that single vehicle to roadside protective facility crash is significant to affect the probability of injury crashes, through the entire freeway sections with horizontal and vertical curve combinations [5]. Alfonso et al. highlighted that the achievement of proper geometric design consistency is a key design element on motorways because of the safety consequences of design inconsistencies [6]. The influence of horizontal and vertical alignment on their traffic operation was studied on 19 uniform segments from Spain; it was proved that deviations on horizontal alignment or longitudinal profile may produce bad estimation if they are not considered on the analysis procedure [7]. The 85th percentile vehicle speed had been adopted as part of geometric design consistency evaluation criteria [8].

The rapid change rate of lateral acceleration may introduce large amplitude jumps [9]. Shu et al. found that critical safety driving speed on lower standard rural roads can be obtained by balancing the design parameters of adjacent curve radii and the tangent length in-between, as the use of hairpin curves and the absence of spirals would lead to a rapid increase in both angular speed of steering wheel and lateral acceleration change rate [10]. MISRO et al. summarized curvature information of Bezier curve for the purpose of approximating maximum speed on a highway, and they

utilized verification between heuristic method and Bezier method to estimate the maximum allowed speed [11].

Yan et al. established an alignment description model based on the principle of spatial geometry, and they set up the relationship between alignment comprehensive indices and operating speed for continuous prediction. This relationship makes it possible to predict a reliable and continuous operating speed profile at each point along the alignment and to significantly improve the performance of consistency alignment design and safety evaluations [12]. Consistency evaluation method was proposed as a surrogate measure to estimate the safety of a highway segment [13].

Specific speed limit implementation scheme for a multicurve highway section was proposed with an example for mountain highways [14]; however, only curve section was studied. Shin and Lee presented reliability analysis and reliability-based optimization of roadway minimum radius design based on vehicle dynamics, and the performance functions were formulated as failure modes of vehicle rollover and sideslip [15]. Zhou et al. proposed a speed warning scheme for heavy-duty vehicle over the horizon in mountainous area to give the drivers enough time to respond to the danger [16].

In this paper, we study on the safety model considering the consistency of adjacent sections, taking the accident form of steep slope with sharp curve of mountain highway as constraint condition. And we quantitatively give the thresholds of geometric design parameters of the combination sections of SSSC. The above thresholds also provide basis for the design of highways at mountainous area. The roadmap of this paper is shown in Figure 1.

2. Safety Analysis Models

2.1. Steep Slope Condition. Climbing performance of heavy-duty vehicles has been greatly improved with the development of automobile industry. The safety of braking at steep downgrade sections has become a more serious problem to be considered, which is influenced by many factors. A temperature rise model based on energy theory is established.

Assuming the vehicle total mass is m (kg), the gravity is G (N), the slope is α (%), and the slope length is S (m). Relationship of gravitational potential energy, engine drag resistant working, pavement resistant force working, and brake consumption is analysed, energy model of vehicle braking on ramps is built in

$$\mathrm{Q}\,(\mathrm{t}) = \Delta E_H - \Delta E_D - \Delta W_E - \Delta W_F \tag{1}$$

where

Q(t) is the total energy consumed for vehicle braking;

ΔE_H is the change of gravity potential energy, calculated by (2);

and ΔE_D is the change of kinetic energy, calculated by (3).

$$\Delta E_H = G \bullet S \bullet \sin\alpha \tag{2}$$

$$\Delta E_D = 0.5mv_t^2 - 0.5mv_0^2 \tag{3}$$

where v_0 is the initial speed of vehicle; v_t is the speed at the bottom of the slope; W_E is the total work done because of all kinds of resistance for downhill driving; W_F is the work done for engine braking, which can be obtained by engine braking tests.

W_F is neglected for simplifying the model calculation, as the relative research shows that W_F has little proportion in braking work [5].

The resistance force of a vehicle in the downhill running mainly includes aerodynamic drag and rolling resistance, shown in (4).

$$W_E = \Delta W_A + \Delta W_R \tag{4}$$

where W_A is the air resistance work, calculated by (5);

$\overline{F_w}$ is the average air resistance, calculated by (6);

K is the air resistance coefficient;

S is the windward area; $\overline{v}$ is the average vehicle speed of the slope (m/s);

W_R is the rolling resistance work, calculated by (7);

$S_\emptyset$ is the brake slip rate of the vehicle; and f is the rolling resistance coefficient.

$$\Delta W_A = \overline{F_w} \bullet S \tag{5}$$

$$\overline{F_w} = \frac{KA\overline{v}^2}{21.15} \tag{6}$$

$$\Delta W_R = G \bullet f \bullet \cos\alpha \bullet S \bullet (1 - S_\emptyset) \tag{7}$$

Then, the total energy consumed during downhill braking is shown in

$$\begin{aligned}\Delta \mathrm{Q}\,(t) = {} & G \bullet S \bullet \sin\alpha - \left(\frac{1}{2}mv_t^2 - \frac{1}{2}mv_0^2\right) \\ & - \left(G \bullet f \bullet \cos\alpha \bullet S \bullet (1 - S_\emptyset) + \overline{F_w} \bullet S\right)\end{aligned} \tag{8}$$

The total energy consumed by the brake will be distributed between the brake and the tire, and part of the heat consumed by the brake will be converted to heat energy of temperature rise. The rest will be dissipated in the form of heat convection, heat radiation, and so on, the brake absorbs ratio p (shown in (9)) which can be used to characterize this part [17].

$$p = 1 - e^{-0.424\overline{v}} \tag{9}$$

Therefore, the temperature rise models of front and rear wheel brake are shown in

$$\left\{\begin{array}{c} \Delta T_F = \dfrac{(\beta_D/2)(1 - S_\emptyset) \bullet \Delta Q\,(t)}{m_F \bullet C} \bullet p \\ \Delta T_R = \dfrac{((1 - \beta_D)/2)(1 - S_\emptyset) \bullet \Delta Q\,(t)}{m_R \bullet C} \bullet p \end{array}\right\} \tag{10}$$

where β_D is the partition coefficient of the braking force, m_F is the mass of the front brake, m_R is the mass of the rear brake, and C is the specific heat capacity of the brake.

In order to ensure the brake work, the maximum temperature must be limited. It was shown that the braking efficiency

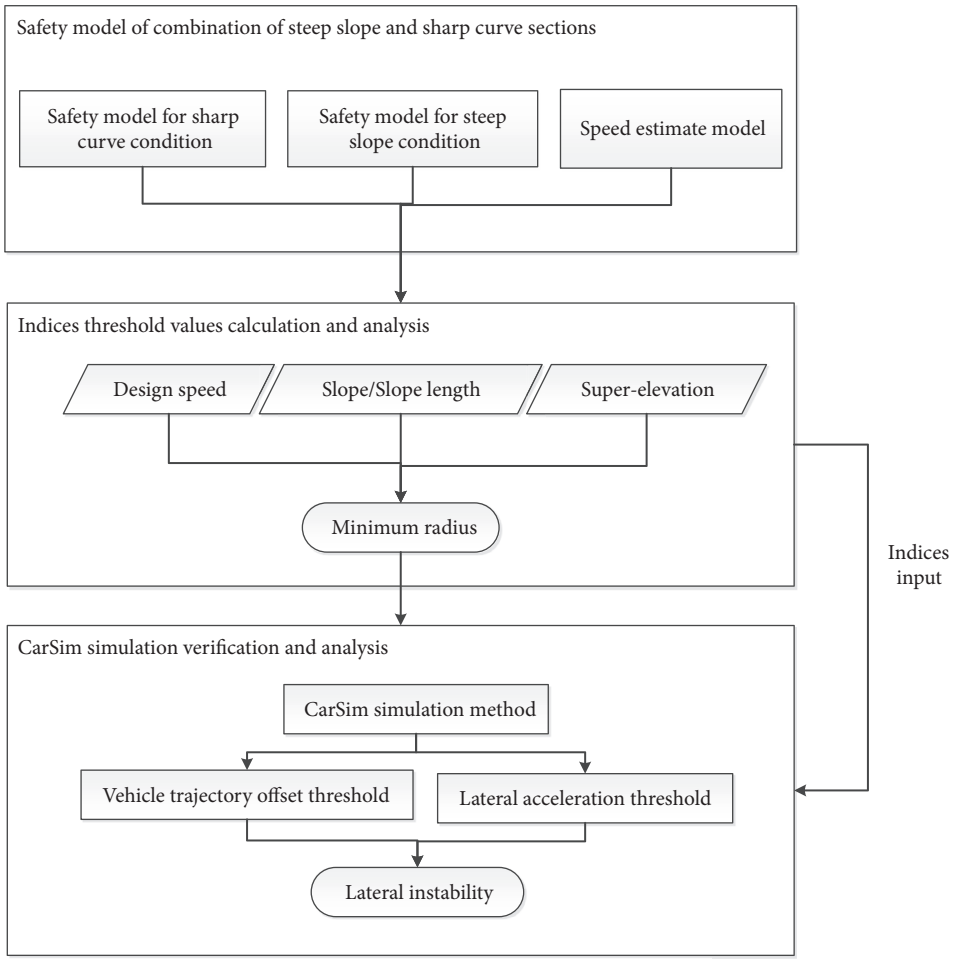

Figure 1: Roadmap of this paper.

is not affected when the brake temperature is generally less than 200°C [18], the thermal fading phenomenon begins to appear when the brake temperature is about 300°C, and the braking force almost disappears when the brake temperature reaches 600°C. From the point of view of ensuring the safety of vehicle braking, the allowable maximum temperature is set as 250°C; slope length can be calculated by

$$\left\{\begin{array}{l} S_{Fmax} \le \dfrac{\left(2 \bullet \Delta T_F \bullet m_F \bullet C\right) / \left(\beta_D \left(1 - e^{-0.424\overline{v}}\right)\left(1 - S_\emptyset\right)\right) + (1/2)\, mv_t^2 - (1/2)\, mv_0^2}{G \bullet \sin\alpha - G \bullet f \bullet \cos\alpha \bullet \left(1 - S_\emptyset\right) - KA\overline{v}^2/21.15} \\ S_{Rmax} \le \dfrac{\left(2 \bullet \Delta T_R \bullet m_R \bullet C\right) / \left(1 - \beta_D\right)\left(1 - e^{-0.424\overline{v}}\right)\left(1 - S_\emptyset\right) + (1/2)\, mv_t^2 - (1/2)\, mv_0^2}{G \bullet \sin\alpha - G \bullet f \bullet \cos\alpha \bullet \left(1 - S_\emptyset\right) - KA\overline{v}^2/21.15} \end{array}\right\} \tag{11}$$

where S_{Fmax} is the maximum slope length ensuring work of the front wheel brake and S_{Rmax} is the maximum slope length ensuring work of the rear wheel brake.

The accumulative temperature rise of brake can be regarded as the sum of the temperature rise of each section when the vehicle is running in the continuous steep sections with different slopes; the constraint equations are shown in

$$\Delta T_{Fmax} \ge \Delta T_F = \sum_{i=1}^{n} \Delta T_{Fi} \tag{12}$$

$$\Delta T_{Rmax} \ge \Delta T_R = \sum_{i=1}^{n} \Delta T_{Ri} \tag{13}$$

2.2. Sharp Curve Condition. We choose longitudinal motion, lateral motion, yaw motion, and four wheel steering motions to study the driving stability by a seven-degree-of-freedom vehicle analysis model. The force analysis of the vehicle is shown in Figure 2.

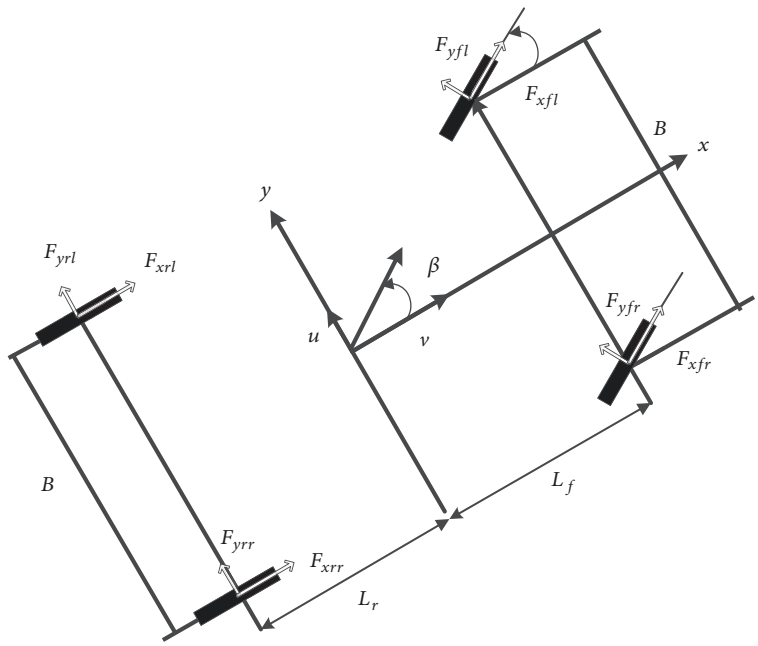

Figure 2: Force analysis of vehicle on curves.

The direction the vehicle runs in is x axle and the vertical direction is y axle; v is the longitudinal velocity; u is the lateral velocity; γ is the yaw angular velocity; δ is the front wheel angle; m is the total mass (kg) of the vehicle; L_f is the front axle and L_r is the rear axle; F_{xfl} is the longitudinal force of the left front wheel; F_{yfl} is the lateral force of the left front wheel; F_{xfr} is the longitudinal force of the right front wheel; F_{yfr} is the lateral force of the right front wheel; F_{xrl} is the longitudinal force of the left rear wheel; F_{yrl} is the lateral force of the left rear wheel; F_{xrr} is the longitudinal force of the right rear wheel; F_{yrr} is the lateral force of the right rear wheel; and B is the wheel spacing.

The vertical force of each tire is different under different driving conditions. The ground support force of the tire is equal to the vertical load of the tire if the mass of the tire is neglected. "Dugoff" tire model [19] is used for calculating the vertical dynamic load with the acceleration, steering, braking, and other driving conditions, shown in

$$\begin{Bmatrix} F_{zfl} = \frac{m}{L}\left(\frac{l_r\left(g \bullet \cos\beta + \dot{u} \bullet \sin\beta\right)}{2} - \frac{\dot{v}h_g}{2} - \frac{l_r\left(\dot{u}h_g \bullet \cos\beta - gh_g \bullet \sin\beta\right)}{B}\right) \\ F_{zfr} = \frac{m}{L}\left(\frac{l_r\left(g \bullet \cos\beta + \dot{u} \bullet \sin\beta\right)}{2} - \frac{\dot{v}h_g}{2} + \frac{l_r\left(\dot{u}h_g \bullet \cos\beta - gh_g \bullet \sin\beta\right)}{B}\right) \\ F_{zrl} = \frac{m}{L}\left(\frac{l_f\left(g \bullet \cos\beta + \dot{u} \bullet \sin\beta\right)}{2} - \frac{\dot{v}h_g}{2} - \frac{l_f\left(\dot{u}h_g \bullet \cos\beta - gh_g \bullet \sin\beta\right)}{B}\right) \\ F_{zrr} = \frac{m}{L}\left(\frac{l_f\left(g \bullet \cos\beta + \dot{u} \bullet \sin\beta\right)}{2} - \frac{\dot{v}h_g}{2} + \frac{l_f\left(\dot{u}h_g \bullet \cos\beta - gh_g \bullet \sin\beta\right)}{B}\right) \end{Bmatrix} \quad (14)$$

The side slip phenomenon of the tire and the acceleration/deceleration state of the vehicle both affect the vertical load of the tire. Suppose the vehicle is running at uniform speed at the curve; (14) can be simplified to (15) ($\dot{v} = 0$, $\dot{u} = F_g/m$, $l_r + l_f = L$).

$$\begin{Bmatrix} F_{zfl} = \frac{l_r}{L}\left(\frac{\left(G \bullet \cos\beta + F_g \bullet \sin\beta\right)}{2} - \frac{\left(F_g h_g \bullet \cos\beta - Gh_g \bullet \sin\beta\right)}{B}\right) \\ F_{zfr} = \frac{l_r}{L}\left(\frac{\left(G \bullet \cos\beta + F_g \bullet \sin\beta\right)}{2} + \frac{\left(F_g h_g \bullet \cos\beta - Gh_g \bullet \sin\beta\right)}{B}\right) \\ F_{zrl} = \frac{l_f}{L}\left(\frac{\left(G \bullet \cos\beta + F_g \bullet \sin\beta\right)}{2} - \frac{\left(F_g h_g \bullet \cos\beta - Gh_g \bullet \sin\beta\right)}{B}\right) \\ F_{zrr} = \frac{l_f}{L}\left(\frac{\left(G \bullet \cos\beta + F_g \bullet \sin\beta\right)}{2} + \frac{\left(F_g h_g \bullet \cos\beta - Gh_g \bullet \sin\beta\right)}{B}\right) \end{Bmatrix} \quad (15)$$

When a vehicle is in a rollover critical state, the vertical loads of the two wheels inside the vehicle are $F_{zfl} = 0$ or $F_{zrl} = 0$.

In order to avoid rollover instability, the minimum radius must be satisfied by

$$R_{fmin} = \frac{v^2\left(2h_g - B \bullet \tan\beta\right)}{g\left(B + 2h_g \bullet \tan\beta\right)} \quad (16)$$

When a vehicle is in a critical state of sideslip, any lateral force on its front and rear axles is equal to the lateral adhesion force: $F_{hl} = (F_{zfl} + F_{zfr}) \bullet \varphi$ or $F_{hr} = (F_{zrl} + F_{zrr}) \bullet \varphi$.

To avoid sideslip instability, the minimum radius must be satisfied by

$$R_{hmin} = \frac{v^2\left(1 - \varphi \bullet \tan\beta\right)}{g\left(\varphi + \tan\beta\right)} \quad (17)$$

where φ is the lateral adhesion coefficient, which is related to the type of pavement, and $\varphi \geq 0.15$ can satisfy various pavement conditions considering driving safety.

To ensure the vehicle not undergo lateral instability in the curve section, the minimum radius should be satisfied by

$$R_{min} \geq \max\left(R_{fmin}, R_{hmin}\right) \quad (18)$$

2.3. Continuity Model for SSSC. A vehicle tends to be faster and prone to lateral instability on the curve when the vehicle enters a sharp curve from a steep slope. It is necessary to take the steep slope segment and curve segment as a whole for safety analysis. Taking the bottom of the slope as the critical point which connects the two segments, the slope length of the first segment is demand less than the maximum slope length. The design index of the rear segment is determined by the operating speed of the slope bottom and the stability of the vehicle in the curve segment, so as to ensure the continuity and safety of the front and rear segments, shown in

$$\left\{\begin{array}{l} S_{max} \le \min\left(S_{Fmax}, S_{Rmax}\right) \\ R_{min} \le \max\left(R_{fmin}, R_{hmin}\right) \end{array}\right\} \tag{19}$$

where

S_{max} is the maximum slope length to insure brake work during the steep slope; S_{Fmax}, S_{Rmax} are calculated by (11);

R_{min} is the minimum allowable radius for the rear alignment unit without lateral instability; R_{fmin}, R_{hmin} are calculated by (16) and (17).

3. Operating Speed Estimation Models

3.1. Speed Estimation for Slope Segment. Operating speed is the key to connect the design indices of the adjacent alignment units. We use the force balance equation of vehicles running on a longitudinal slope to calculate the operating speed, shown in

$$\left\{\begin{array}{c} (f+a)\, gvm + KFv^3 + \delta vma - \overline{P_U} = 0 \\ a = \dfrac{\overline{P_U}}{\delta vm} - \dfrac{(f+a)\, g}{\delta} - \dfrac{KFv^2}{\delta m} \end{array}\right\} \tag{20}$$

Assuming the acceleration or deceleration is uniform during the process of changing speed due to linearity in running, the velocity of the vehicle at any point on the longitudinal slope can be solved by

$$\frac{\overline{P_U}}{m} - \left(\frac{v_t + v_0}{2}\right)\left[(f+a)\, g + \frac{KF\left(\left(v_t + v_0\right)/2\right)^2}{m} + \left(1+\delta_1\right)\left(\frac{{v_t}^2 - {v_0}^2}{2S}\right)\right] = 0 \tag{21}$$

where f is rolling resistance coefficient; a is the slope; m is the vehicle mass; K is wind resistance coefficient; F is windward area; $\overline{P_U}$ is average power; δ_1 is inertial force influence coefficient of vehicle (between 0.03 and 0.05).

As the estimated operating speed of steep slope should not exceed the expected speed of the highway section, if the calculated operating speed at a certain point is higher than the expected speed of the highway section, the expected speed is used as the initial speed of the end of the slope (the initial speed of the curve), although people may not follow the expected speed in actual driving behaviour.

3.2. Speed Estimation for Curve Section. According to standard of safety assessment of highway projects [3], the operating speed should be coordination evaluated for highways if the design speed is lower than 80 km/h. The circular curve model is used to estimate the operating speed of the curve sections, shown in Table 1.

v_1 is the speed at the starting point of curve, v_2 is the estimated speed at the middle point of curve, v_3 is the estimated speed at the end of curve, R_{now} is the radius of the circular curve of the highway section, and R_{front} is the radius of the next curve segment.

For small vehicle, if R_{front} is greater than five times R_{now}, then $R_{front} = 5R_{now}$. For large vehicle, R_{front} is greater than four times R_{now}, then $R_{front} = 4R_{now}$.

The speeds of the initial point, the midpoint, and the end point of the curve are calculated according to operating speed estimation model for curve sections, and he maximum speed is used for checking the minimum radius (shown in (22)).

$$\mathrm{R} \ge \frac{v_i^2\left(1 - \varphi\tan\beta\right)}{g\left(\varphi + \tan\beta\right)} \quad (i = 1, 2, 3) \tag{22}$$

According to the speed estimation model in Table 1, the speed of the vehicle at the initial point of the curve is greater than the speed of the midpoint of the curve; especially the adjacent section between straight line to circular curve; the speed is increased at the latter half of the curve. And operating speed at any point of the curve should not be higher than the expected speed.

4. Simulation Method

CarSim simulation software is used to simulate and demonstrate the coordinated relationship between the design parameters of combination of SSSC.

The main factors that affect the safety of vehicles on steep slopes and sharp curves are side slip or rollover of vehicles at the bottom of the slope, which can be judged by analysis of vehicle steering operation stability. Trajectory offset, tire vertical counterforce, and lateral acceleration are used as the simulation indices. We recorded trajectory offset and lateral acceleration in the simulation to reflect driving stability. Relevant study shows that lateral instability may occur when vehicle trajectory deviation exceeds 0.3 m or lateral acceleration reaches 0.3 g [20]. In this simulation, we use trajectory offset and lateral acceleration to indirectly express the degree of lateral instability, and the results are compared to verify the effectiveness of the simplified safety model established.

In order to ensure the coordination of the geometry, the ratio of the lengths of gyroscopic line, circular curve and gyroscopic line is designed to be 1:1:1. The "X-Y-Z coordinates of edges method" is used in CarSim software to establish a three-dimensional geometry model of highway, which is similar to the current highway design method. The procedure of the modelling is as follows: firstly, determine the direction and three-dimensional coordinates of the midline, then use

Table 1: Estimation model of operating speed of double lane highway in mountain area [3].

Small vehicle	Midpoint of curvature	$v_2 = -244.123 + 0.6v_1 + 40\ln(R_{now} + 500)$
	Curvature point	$v_3 = -183.092 + 0.7v_2 + 30\ln(R_{front} + 500)$
Large vehicle	Midpoint of curvature	$v_2 = -80.179 + 0.7v_1 + 15\ln(R_{now} + 250)$
	Curvature point	$v_3 = -53.453 + 0.8v_2 + 10\ln(R_{front} + 250)$

Figure 3: Road model.

the midline as the axis, expand on both sides to get a three-dimensional highway model according to the superelevation; the highway model is shown in Figure 3.

Since the road model, the vehicle model (C-Class vehicle model built in CarSim software), and the driver model (fixed speed) are all programmed, the simulation is reproducible, a determined model only needs to be simulated once. Assume radius between 15 m and 500 m corresponds to various road models with superelevation between 0 and 10%. The maximum speed of the critical condition of side slip is obtained by debugging on different road models, and the mathematical relationship between the maximum speed and the corresponding design parameters of highways is established.

5. Results and Discussion: Geometric Design Indices Calculation and Simulation Verification

5.1. Geometric Design Indices Calculation. According to the statistics data of 456 traffic accidents on curved highways (14505 accidents in total) on highways of Chongqing city in 2014, 66% were small buses, 17% were small trucks, and 17% were large trucks [1]. We chose small buses and large trucks for this study, and typical representative vehicles of small buses and large trucks are set as Buick Regal and FOTON ROWOR (vehicle models built in CarSim software), respectively; parameters of the two types of vehicles are shown in Table 2.

The maximum slope length under different design speed is taken as the parameter of the first unit, and the operating speed at the bottom of the slope is calculated as the speed at initial point of the curve. The minimum radius with different superelevations is calculated according to (14), and calculations of the two types of vehicles are shown in Tables 3 and 4, respectively.

The following can be seen from Tables 3 and 4:

(i) There is a negative correlation between the minimum radius of the second segment and the superelevation of the curve; on the contrary, the correlation between the design speed and the minimum radius of the second segment is positive. And the increase rate of the minimum radius grows as the speed is higher.

(ii) When the longitudinal slope of the first segment is 6% and the superelevation of the second segment is 4%, the design speed for large vehicles increases from 20 km/h to 80 km/h; the minimum radius of the second segment (curve section) increases from 26 m to 264 m. Therefore, more attention should be paid to the geometry coordination of steep slope and curve section with high design speed, and the small radius curve connected to steep slope should be avoided.

(iii) The minimum radius of the second segment is negative related to the gradient of the first segment. However, when design speed is lower than 40 km/h, the change of slope and slope length has little effect on the speed of vehicle at the bottom of the slope and has little effect on the minimum radius of the second segment.

(iv) The minimum radius of the second segment calculated with large vehicle model is smaller than that calculated with small vehicle model, as the estimated operating speed of the small vehicle is generally higher than that of the large vehicle.

(v) As the minimum radius is positive related to the speed of the vehicle, so small vehicles are prone to accidents on SSSC section. Therefore, the speed limit measures should be taken into consideration in the design of steep slope sections.

5.2. Simulation Verification and Analysis

5.2.1. Superelevation. The parameters are set as follows: the slope of the first segment is 4%; the slope length of the

Table 2: Vehicle model parameters.

Vehicle type	Small vehicle (Buick Regal)	Large vehicle (FOTON ROWOR)
Mass (kg)	1390	11570
Front wheel brake disc / drum quality (kg)	4.9	15.52
Rear wheel brake disc / drum quality (kg)	9.36	19.80
Rolling resistance coefficient f	0.0125	0.0125
Braking force distribution coefficient β	0.56	0.77
Specific heat capacity of brake (j/kg.°C)	470	470
Braking slip ratio S_ϕ	0.1	0.1
Windward area F (m^2)	1.5	6
Drag coefficient of wind K	0.32	0.75
Maximum power (kw)	67	162

Table 3: Minimum radius of the combination section of vertical and horizontal (small vehicle).

Design speed (km/h)	Longitudinal slope (%)	Slope length (m)	Minimum radius (m)		
			4% superelevation	6% superelevation	8% superelevation
20	4	1200	37	33	30
	5	1000	37	33	30
	6	800	37	33	30
	7	600	37	33	30
	8	400	37	33	30
	9	300	37	33	30
	10	200	32	29	26
30	4	1100	66	59	54
	5	900	66	59	54
	6	700	66	59	54
	7	500	66	59	54
	8	300	66	59	54
	9	200	59	54	49
40	4	1100	148	134	122
	5	900	125	112	102
	6	700	103	93	84
	7	500	103	93	84
	8	300	103	93	84
60	3	1200	291	262	238
	4	1000	264	238	216
	5	800	202	182	166
	6	600	202	182	166
80	3	1100	429	386	352
	4	900	396	357	325
	5	700	334	301	274
	6	500	264	238	216

first segment is 1000 m; the limit radius of the second segment is 195 m. The initial speed is set as 60 km/h and the superelevations of the second segment are 4%, 6%, and 8%. The track offsets and lateral accelerations are recorded during the simulations (shown in Figure 4).

The simulation data and graphs show that when the superelevation is 6% or 8%, the maximum lateral offset of the vehicle on the curve section is in the inside direction, and the offset is far less than 0.3 m; the lateral offset difference with different superelevations is little. The lateral accelerations corresponding to the superelevations (4%, 6%, and 8%) are 0.19 g, 0.161 g, and 0.126 g, respectively, so the lateral acceleration shows a clear decreasing trend with the slope increases. This indicates that the vehicle is more stable driving on

Table 4: Minimum radius of the combination section of vertical and horizontal (large vehicle).

Design speed (km/h)	Longitudinal slope (%)	Slope length (m)	Minimum radius (m)		
			4% superelevation	6% superelevation	8% superelevation
20	4	1200	26	23	21
	5	1000	26	23	21
	6	800	26	23	21
	7	600	26	23	21
	8	400	26	23	21
	9	300	26	23	21
	10	200	26	23	21
30	4	1100	50	45	41
	5	900	50	45	41
	6	700	50	45	41
	7	500	50	45	41
	8	300	50	45	41
	9	200	50	45	41
40	4	1100	103	93	84
	5	900	83	75	68
	6	700	83	75	68
	7	500	83	75	68
	8	300	83	75	68
60	3	1200	202	182	166
	4	1000	202	182	166
	5	800	148	134	122
	6	600	148	134	122
80	3	1100	264	238	216
	4	900	264	238	216
	5	700	202	182	166
	6	500	202	182	166

sections with larger turning radius when the superelevation is fixed, and the variation of radius is inversely related to the superelevation.

5.2.2. Vehicle Speed. The parameters are set as follows: the slope of the first segment is 4%, the slope length is 1000 m, the limit radius of the second segment is 195 m, and the superelevation is 4%.

The simulation iteration frequency is 100 Hz (using the target speed control mode). The downhill speeds are set as 40 km/h, 60 km/h, and 80 km/h; track offset and lateral acceleration records are shown in Figure 5.

The simulations show that the maximum lateral offset is 0.046 m inside the curve at the speed of 40 km/h, the maximum lateral offset is 0.028 m inside the curve at the speed of 60 km/h, and the difference between the left and right maximum offset is 0.09 m; the maximum lateral offset is 0.158 m outside the curve at the speed of 80 km/h, and the difference between the left and right maximum offset is 0.18 m. The maximum offset appears inside the curve when entering the curve segment at 40 km/h, which indicates that the vehicle can pass the curve smoothly. When the speed increases from 60 km/h to 80 km/h, the direction of the maximum lateral offset of the vehicle becomes the outside of the curve. The maximum offset of the vehicle at 80 km/h is outside the curve, indicating that the vehicle may have insufficient steering.

The lateral offsets corresponding to 60 km/h and 40 km/h are both far less than 0.3 m, the speed variation is 20 km/h, and the transverse offset difference is 0.018 m. While the lateral offset of the vehicle is 0.158 m at the speed of 80 km/h, the transverse offset difference is 0.12 m. The maximum lateral offset increment of the vehicle increases with the increase of the speed, but it is not a linear growth trend. We can see from the trend that if the speed is further increased, the lateral offset of the vehicle may exceed 0.3 m, and the steering instability may occur. The higher speed of the vehicle, the larger turning radius is needed.

The maximum lateral acceleration of the vehicle is toward the inside of the curve, and the lateral accelerations corresponding to 40 km/h and 60 km/h are 0.079 g and 0.19 g, respectively. They are both less than 3.75 m/s^2, which is the critical value that makes the driver feel uncomfortable. While the lateral acceleration at 80 km/h is about 0.365 g (approximately 3.58 m/s^2), which is very close to the lateral comfort acceleration constraint value (3.75 m/s^2). It can be seen that the comfort and stability of the vehicle have been affected while passing through the curve at the speed

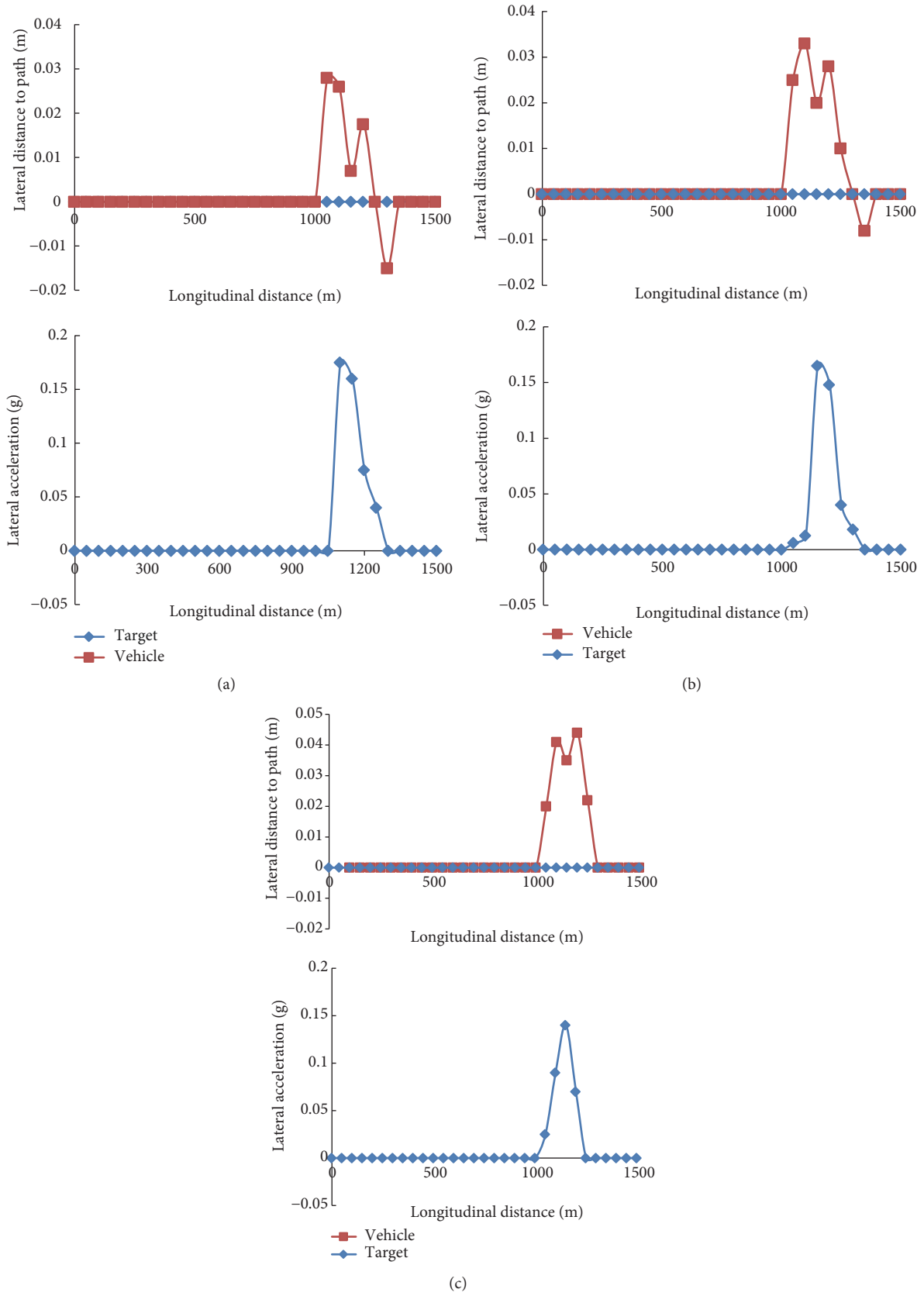

FIGURE 4: The track offset and lateral acceleration of different superelevations. (a) 4% longitudinal slope. (b) 6% longitudinal slope. (c) 8% longitudinal slope.

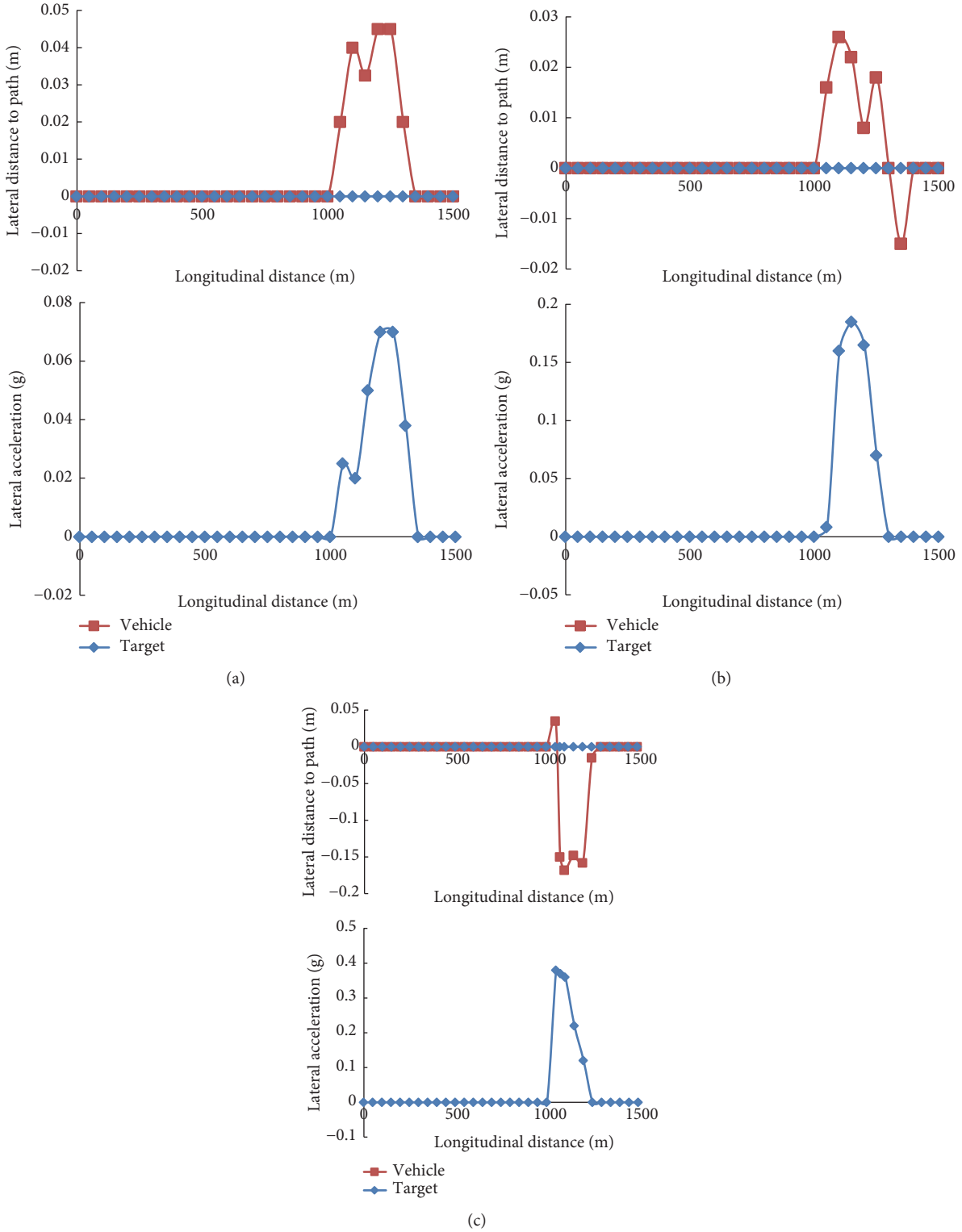

Figure 5: The track offset and lateral acceleration of different vehicle speed. (a) 40 km/h. (b) 60 km/h. (c) 80 km/h.

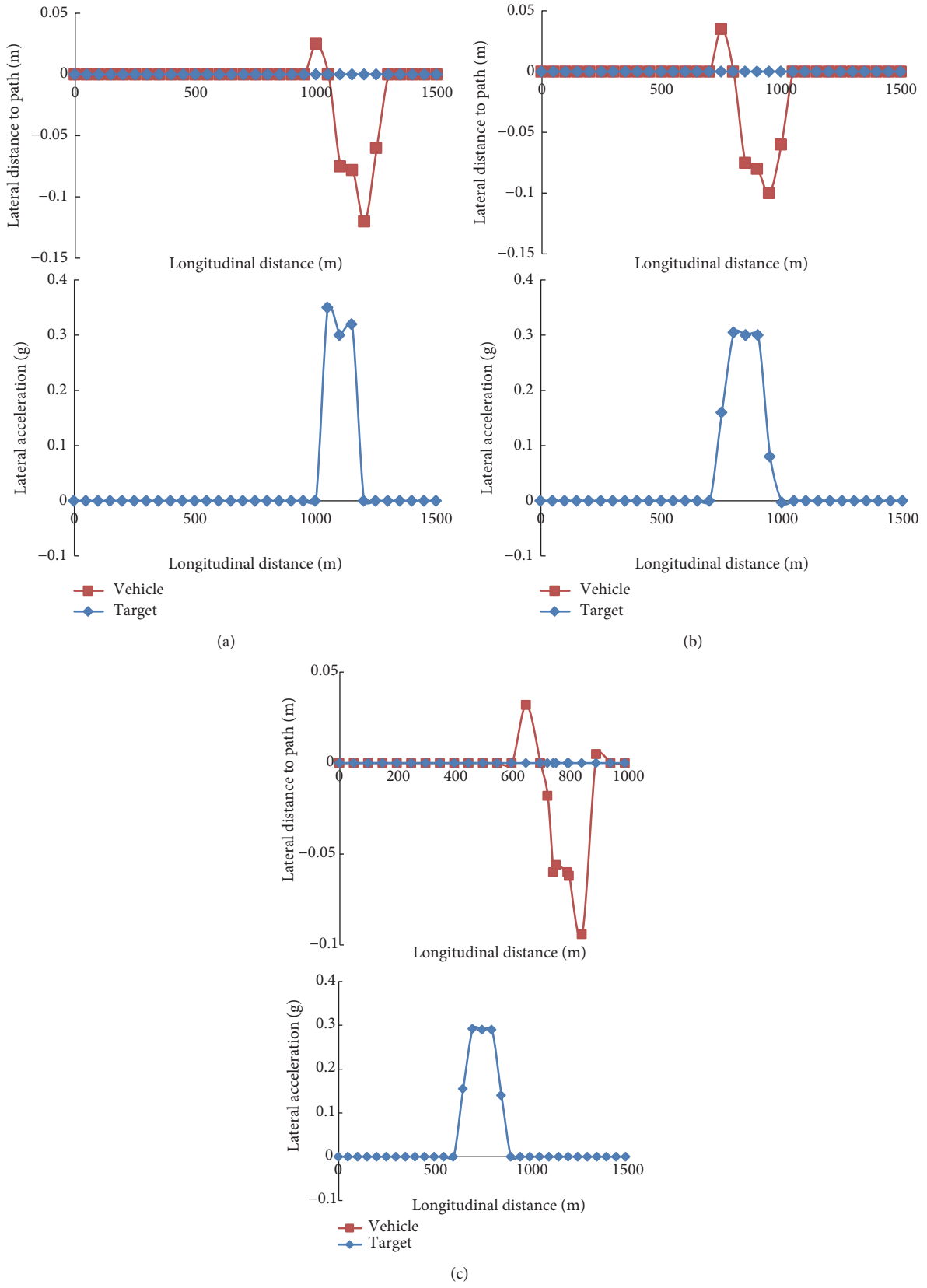

Figure 6: The track offset and lateral acceleration of different slope parameters (a) 4% slope and 1000 m slope length. (b) 5% slope and 800 m slope length. (c) 6% slope and 600 m slope length.

of 80 km/h, so the vehicle needs to slow down passing SSSC section. As the limit radius required to ensure the safety of vehicles on SSSC sections will increase with the increase of speed, it is necessary to slow down to ensure the stability and safety of vehicles when radius of the curve is small.

5.2.3. Slope Length. The initial simulation parameters are set as follows: design speed is 60 km/h, limit radius of the second segment is 195 m, and superelevation is 4%.

The longitudinal slope of 4% corresponds to the slope length of 1000 m, the longitudinal slope of 5% corresponds to the slope length of 800 m, and the longitudinal slope of 6% corresponds to the slope length of 600 m. The track offset and lateral acceleration are recorded in both cases, as shown in Figure 6.

It can be seen from the graphs in Figure 6 that when the slope is 4% or 6%, the maximum lateral offsets of the vehicle on the curve section appear in the outside direction, and values are both around 0.1 m, far less than the prescribed. Therefore, the slope of the first segment and the length of the slope have little effect on the second segment.

The lateral accelerations of the vehicle under the three restriction slope lengths are all around 0.3 g, and the change trend of the lateral acceleration is similar. This also indicates that the restriction slope length of the steep slope segment has little effect on the stability of the vehicle driving on the subsequent curve segment. The main reason is that the limit slope length as the main geometry index of the first segment of steep slope section exceeds the characteristic length of vehicle speed variation in downhill section. In the case of the same initial speed, in the "normal driving route" speed control mode, the vehicle speed tends to be stable at the bottom of the slope. The first segment seems have little effect on the main parameters of the second segment.

6. Conclusions

An overall safety model of SSSC combined section is established based on the analysis of vehicle driving stability, and the relevant coordination relationship between the design indices of the front and rear alignment segments is established by using the operating speed estimation model. Safety model is simulated by CarSim software, which verified the coordination relationship between the design parameters of SSSC sections. The trajectory offset and lateral acceleration are used to indirectly reflect the degree of lateral instability, and the results are compared to verify the effectiveness of the simplified safety model established in this paper.

The minimum radius of the sharp curve of the rear segment is positively related to the design speed and negatively related to the slope and superelevation of the first segment. The effect of the slope of first segment on the minimum radius of the rear segment is not obvious when the design speed is low. Considering the operating speed, the minimum radius of the rear segment should be larger than the minimum radius of the existing regulations, and it is suggested that the minimum radius should be increased and speed restriction measures should be set for sharp curve and steep slope sections.

This paper builds a simplified safety model, discusses optimization design method of SSSC highway sections, and verifies this model by CarSim software with indirect instability indices. The design method and the simulation method are effective.

Further research will be necessary to confirm the operating speed of the curve which has been simply set with desired speed in this study. The influence of other parameters, such as view of driver, should also be considered in the geometry design, which is not included in this paper.

Data Availability

The traffic accidents data used to support the findings of this study have not been made available because of secrecy.

Conflicts of Interest

The authors declare that there are no conflicts of interest regarding the publication of this paper.

Acknowledgments

This work was supported by the National Natural Science Foundation of China under Grant 51708065 and Central College Project of Chongqing University under Grant 106112017CDJXY200006.

References

[1] Chongqing Municipal Transportation Commission, *Report of Analysis of Statistical Data in Transportation Industry*, Chongqing, China, 2014.

[2] Ministry of communications and transportation of People's Republic of China, *Standard of Highway Alignment Design*, JTG D20-2017, China, 2017.

[3] Ministry of communications and transportation of People's Republic of China, *Standard of Safety Assessment of Highway Projects*, JTG B05-2015, China, 2015.

[4] J. Xu, W. Lin, and Y. Shao, "New design method for horizontal alignment of complex mountain highways based on "trajectory-speed" collaborative decision," *Advances in Mechanical Engineering*, vol. 9, no. 4, pp. 1–18, 2017.

[5] S. Jung, K. Wang, C. Oh, and J. Chang, "Development of highway safety policies by discriminating freeway curve alignment features," *KSCE Journal of Civil Engineering*, vol. 22, no. 4, pp. 1418–1426, 2018.

[6] A. Montella and L. L. Imbriani, "Safety performance functions incorporating design consistency variables," *Accident Analysis & Prevention*, vol. 74, pp. 133–144, 2015.

[7] A. T. Moreno, C. Llorca, and A. Garcia, "Operational impact of horizontal and vertical alignment of two-lane highways," *Transportation Research Procedia*, vol. 15, pp. 319–330, 2016.

[8] S. Nama, A. K. Maurya, A. Maji, P. Edara, and P. K. Sahu, "Vehicle speed characteristics and alignment design consistency for mountainous roads," *Transportation in Developing Economies*, vol. 2, no. 2, pp. 2–23, 2016.

[9] N. Massoudian and M. Eshghi, "Design an intelligent curve to reduce the accident rate," in *Proceedings of the 2015 Signal Processing and Intelligent Systems Conference (SPIS)*, pp. 185–188, Amirkabir University of Technology, Tehran, Iran, December 2015.

[10] H.-B. Shu, Y.-M. Shao, W. Lin, and J. Xu, "Computation-based dynamic driving simulation for evaluation of mountain roads with complex shapes. a case study," in *Proceedings of the Green Intelligent Transportation System and Safety, GITSS 2015*, pp. 210–219, Procedia Engineering, China, 2016.

[11] M. Y. Misro, A. Ramli, and J. M. Ali, "Approximating maximum speed on road from curvature information of Bezier curve, World Academy of Science, Engineering and Technology," *International Journal of Mathematical, Computational, Physical, Electrical and Computer Engineering*, vol. 9, no. 12, 2015.

[12] Y. Yan, G. Li, J. Tang, and Z. Guo, "A novel approach for operating speed continuous predication based on alignment space comprehensive index," *Journal of Advanced Transportation*, vol. 1701, pp. 1–14, 2017.

[13] F. J. Camacho-Torregrosa, A. M. Pérez-Zuriaga, J. M. Campoy-Ungría, and A. García-García, "New geometric design consistency model based on operating speed profiles for road safety evaluation," *Accident Analysis & Prevention*, vol. 61, pp. 33–42, 2013.

[14] Z. Xie, "Speed limit safety of expressway curves based on the critical state evaluation model of vehicle side rollover," *Journal of Engineering Science and Technology Review*, vol. 11, no. 1, pp. 109–116, 2018.

[15] J. Shin and I. Lee, "Reliability analysis and reliability-based design optimization of roadway horizontal curves using a first-order reliability method," *Engineering Optimization*, vol. 47, no. 5, pp. 622–641, 2014.

[16] S. Zhou, G. Tan, K. Ji, R. Zhou, and H. Liu, "Over-the-horizon safety speed warning system for heavy-duty vehicle in mountain areas," SAE Technical Paper 2017-01-0091, 2017.

[17] Yi. Liu, *The Research of Mountain Area Road Longitudinal Design Theory Based on Vehicle-Road Coupling Safety Evaluation Model*, Chongqing Jiaotong University, Chongqing, China, 2017.

[18] K. Zhao, *Study on the Brake's Heat-Fade Performance and Corresponding Braking Safety Detection of Vehicle*, Chang'an University, Xi'an, China, 2010.

[19] H. Dugoff, P. S. Fancher, and L. Segel, "An analysis of tire traction properties and their influence on vehicle dynamic performance," SAE Technical Paper 700377, 1970.

[20] L. Fan, L. Lu, W. Deng, and J. J. Lu, "Role of vehicle trajectory and lateral acceleration in designing horizontal curve radius of off-ramp: a driving simulator based study," *Advances in Transportation Studies an international Journal Section B*, vol. 36, pp. 119–132, 2015.